



NUMERICAL SIMULATION WITH FIBRE BEAM-COLUMN MODELS OF THIN RC COLUMN BEHAVIOUR UNDER CYCLIC TENSION-COMPRESSION

A. Rosso⁽¹⁾, J.P. Almeida⁽²⁾, K. Beyer⁽³⁾

- ⁽¹⁾ PhD candidate, Earthquake Engineering and Structural Dynamics Laboratory (EESD), School of Architectural, Civil and Environmental Engineering (ENAC), École Polytechnique Fédérale de Lausanne (EPFL), Switzerland, angelica.rosso@epfl.ch
- ⁽²⁾ Post-doctoral Researcher, Earthquake Engineering and Structural Dynamics Laboratory (EESD), School of Architectural, Civil and Environmental Engineering (ENAC), École Polytechnique Fédérale de Lausanne (EPFL), Switzerland, joao.almeida@epfl.ch
- ⁽³⁾ Assistant Professor, Earthquake Engineering and Structural Dynamics Laboratory (EESD), School of Architectural, Civil and Environmental Engineering (ENAC), École Polytechnique Fédérale de Lausanne (EPFL), Switzerland, katrin.beyer@epfl.ch

Abstract

Damage to structural walls in the recent earthquakes in Chile (2010) and New Zealand (2011) demonstrated that modern reinforced concrete (RC) wall behaviour can be largely governed by out-of-plane displacements triggered by instability. Thin walls are the most vulnerable to this deformation mechanism, especially if they have a single layer of reinforcement. These wall types can be easily found in some Latin American countries such as Colombia, with minimum thicknesses as low as 8 cm. Relatively little is known about the response of these members, mainly due to the lack of experimental testing and numerical simulations.

The out-of-plane buckling of RC walls is often studied by idealizing the boundary element—which represents the part of the wall mainly involved in the instability mechanism—as an equivalent column axially loaded in tension and compression. This is also the approach followed in the present paper. Further, past experimental campaigns identified the magnitude of the maximum applied tensile strain prior to subsequent loading in compression as the key parameter that triggers the out-of-plane instability. In order to study the effect of this and other variables—e.g., loading history, thickness, and reinforcement ratio—on the out-of-plane response, efficient modelling techniques are required. Such a numerical simulation is challenging because of the need to account for a complex interaction between nonlinear geometric and material effects. The present study illustrates the application of a beam-column model to simulate the out-of-plane response of equivalent columns, representative of the boundary elements of a wall as mentioned above.

In the present work, the response of the beam-column model is first described and discussed in detail. Secondly, the simulation accuracy is assessed by comparison against experimental results from a campaign on equivalent RC columns with a single vertical reinforcement layer that is ongoing at École Polytechnique Fédérale de Lausanne. The results show that the numerical model provides a good estimate, although slightly non-conservative, of the maximum out-of-plane displacement attained and of the maximum tensile strain that causes out-of-plane failure. Finally, the model is used to simulate the out-of-plane response of the boundary element of a thin wall with a single layer of reinforcement tested in the past. This work shows that such a numerical model is a relatively simple tool yet reliable for assessing the vulnerability of thin RC walls to out-of-plane instability.

Keywords: out-of-plane instability of RC members; thin RC walls; beam-column model; numerical simulation.

1. Introduction

Recent earthquakes in Chile (2010) and New Zealand (2011) have shown that, despite many years of extensive research and subsequent design code advancements, many reinforced concrete (RC) walls underperform during

seismic events [1,2]. In fact, many of the observed structural failures are not yet completely understood [3,4]. In some cases, a lateral instability of a large portion of walls was detected, which corresponds to a buckling type of failure that had been observed primarily in laboratory tests [5]. These issues deserve thorough investigations to ensure a satisfactory performance of walls in future earthquakes.

For a wall with double layer reinforcement, the mechanism can be summarised as follows [6,7]: at large in-plane curvature demands the boundary element develops large tensile strains that cause wide near-horizontal cracks across the width of the wall and yielding of the longitudinal reinforcement in tension. Upon unloading, an elastic strain recovery takes place, but due to the plastic tensile strains accumulated in the rebars, the cracks remain open. When reloading in compression and before crack closure, the compression force is resisted solely by the two layers of vertical reinforcement. As long as the rebars retain their significant axial stiffness before yielding in compression, the out-of-plane displacements, which can arise because of construction misalignments in the position of the longitudinal reinforcements or eccentricity of the resultant force acting in this region, tend to remain small. However, as compression increases, the longitudinal rebar near the concave side (intrados of the out-of-plane deformed profile) may yield, leading to an abrupt reduction in out-of-plane stiffness and a consequent increase in the corresponding displacements. At this point, the second layer of longitudinal reinforcement—which has not yet yielded in compression—is the main source of out-of-plane stiffness. For RC walls with a single layer of reinforcement such a restraint does not exist leading hence to a much lower out-of-plane stiffness and larger out-of-plane displacements. Depending on the magnitude of the tensile strain previously attained (i.e., before unloading), different scenarios can then take place as compression progresses [7,8]: the cracks may close, re-establishing compressive force transfer through concrete and contributing to straighten up the wall (at least up to concrete compression crushing), or they may remain open leading to compression yielding of the second layer of reinforcement. In the latter case, out-of-plane displacements will abruptly increase, possibly leading to wall buckling failure. Following the previous rationale, the potential for out-of-plane buckling of walls has been shown to depend foremost on the maximum inelastic tensile strain in the vertical wall edge regions [7,9], which has been since adopted as the engineering demand parameter that best describes the likelihood of onset of lateral wall instability.

The existing models developed to describe the out-of-plane buckling of RC walls [7,8] assimilate the boundary element—which represents the part of the wall mainly involved in the instability mechanism—to an equivalent column axially loaded in tension and compression. In order to study the influence of several variables—such as the loading protocol, the thickness of the specimens, the reinforcement ratio—on the out-of-plane response, efficient modelling techniques are required. The corresponding numerical simulation is challenging because of the need to account for a complex interaction between nonlinear geometric and material effects. The present study illustrates the application of a beam-column model to describe the out-of-plane response of equivalent columns subjected to cyclic tensile and compressive loading.

The numerical model has been used to simulate three experiments performed at École Polytechnique Fédérale de Lausanne, in which equivalent columns with a single layer of reinforcement were tested under cyclic tensile-compressive loading. A preliminary comparison of the results shows that the model can provide an estimate of the maximum tensile strain that caused the out-of-plane failure and a quite accurate description of the development of the instability. Finally, the numerical model was used to simulate the response of a thin wall with a single layer of reinforcement.

2. Numerical simulation

2.1 Description of the numerical model

The 2D beam-column model, representative of boundary elements of thin RC walls, was implemented by the authors to carry out finite element simulations using the software OpenSees [10]. The analyses of a column subjected to axial tension-compression might seem simple at first but are in fact quite challenging because of several issues that may hinder convergence : (i) the sudden drop in concrete tensile strength throughout the section; (ii) the fact that when the section is entirely cracked the only axial and flexural source of

stiffness/strength is provided by the rebars; (iii) the asymmetry of the section, which creates a variable out-of-plane moment along the height due to the geometric nonlinear effects, and the imposed boundary conditions.

Two sources of nonlinearities are considered: (i) material: force-based elements are used (with five Gauss-Lobatto integration points) and the section is discretized into concrete and reinforcement fibres to which nonlinear uniaxial stress-strain laws are assigned; (ii) geometric: these effects are accounted for by using a corotational transformation—to consider the effect of large displacements—and by discretizing the column into several elements along the height, thus simulating the ‘small P-delta’ effect.

The column is discretized into multiple elements along the height and it is fixed at the extremities (see Fig. 1a). These boundary conditions differ from the pin-pin case usually assumed in the existing phenomenological models [7,8], but they better represent the real boundary conditions of the test. Besides, considering the extremities as pin-pin in a column where fibres are used to model an eccentric rebar brings about several problems. In fact, since no reaction moments can be developed at the extremities, when a tensile positive displacement is imposed the equilibrium of the internal moment (which has to be null) at the extremity sections must be achieved through the development of compressive stresses in the extreme concrete fibres on the same side of the section where the bar is placed. Very significant positive curvatures at the extremities have thus to be developed, causing a very large out-of-plane deformation of the column. This behaviour is not representative of the behaviour observed in tests. Hence, the assumption of two fixed restraints at the base and at the top allows for, on the one hand, to realistically equilibrate the internal moments at the extremities and, on the other, to have a better description of the real boundary conditions.

Both the concrete section and the steel bars are discretized in many fibres (see Fig. 1a). The reason why the bar is also divided into several fibres is explained in the following. When the column is subjected to axial loading, the axial force is approximately constant while the bending moment varies along the height of the column (in particular when second order effects become relevant). When the cracks are open over the entire width of the column, such variable internal forces along the height are equilibrated solely by the rebars, which implies that these are required to develop a resisting bending moment. It is therefore necessary to discretize each rebar into several fibres and not only in one, which is the usual procedure when modelling reinforced concrete sections using fibre discretisation.

2.2 Qualitative response of the numerical model

In the following, the results of the numerical simulation are presented and discussed in a qualitative manner, showing a case in which a large out-of-plane deformation is attained and then recovered. The column is subjected to a single cycle of loading, applying first a tensile displacement such that yielding of the total cross-section of the rebar is attained, following by unloading until a certain compressive displacement is reached.

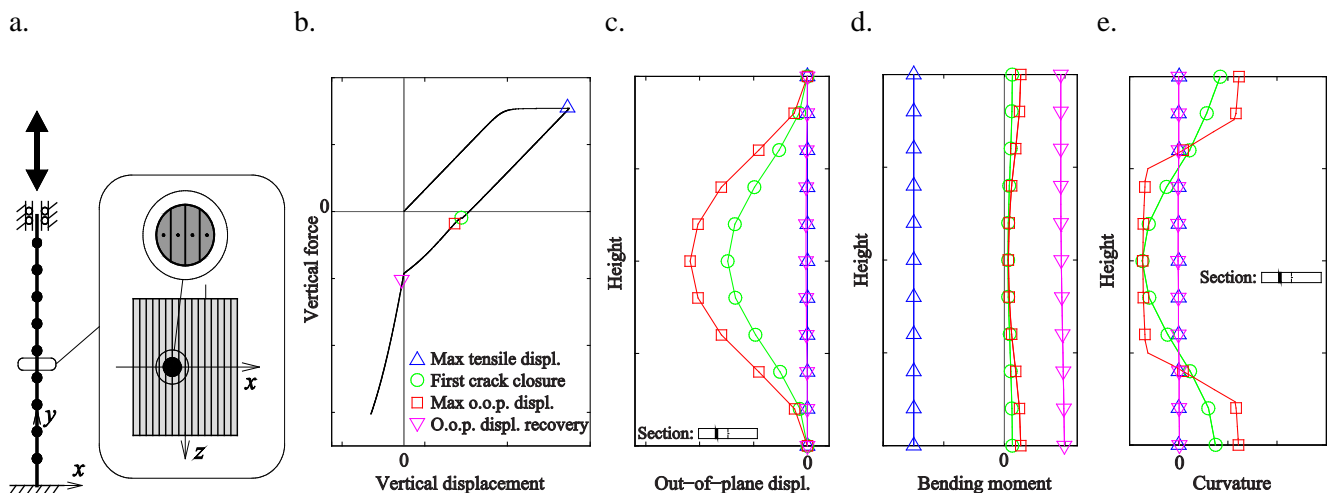


Fig. 1 – a. Illustration of the model; b. Vertical force-displacement response of the model; Profile along the height of c. the out-of-plane displacement, d. the bending moment, and e. the curvature.

Fig. 1b depicts the vertical force-displacement response of the unit, showing that a plastic deformation has occurred. For different values of imposed vertical displacement, the out-of-plane displacement (Fig. 1c), the bending moment (Fig. 1d), and the curvature profiles (Fig. 1e) are reported. Fig. 1c shows that, after attaining a large out-of-plane displacement, the latter is almost completely recovered. Moreover, from Fig. 1b it can be noted that the maximum out-of-plane displacement occurs just after attaining a compressive value of the vertical force, i.e. in the reloading phase, when the vertical displacement is still positive (red squares in Fig. 1b-c). This evidence was noted already in past experimental campaigns on RC walls [5,6,11].

When the maximum tensile displacement is imposed (blue triangles in Fig. 1b to e), the global bending moment is negative, and the out-of-plane displacement and the curvature are almost null. Upon reloading, the bending moment turns to positive and is smaller in the sections experiencing large lateral displacements, i.e. around the column midheight, due to second order effects. When the vertical displacement reduces—see green circles in Fig. 1b to e—the strain in the concrete fibres at midheight reaches a value of zero, indicating that the cracks start closing on the concave side of the deformed shape (i.e., in the section side opposite to the rebar). Upon further reloading, the out-of-plane deformation and the bending moment keep increasing; it can be observed that the minimum value of the curvature is attained at midheight, while a maximum value is reached at the extremities, indicating that the cracks have started closing on the opposite side of the section (i.e., in the same section side of the rebar). When the column is further compressed—red squares in Fig. 1b to e—the out-of-plane displacement is at its maximum. Closure of additional cracks causes an increase of the out-of-plane stiffness of the column, triggering a straightening of the column with consequent reduction of the curvature. By the time the imposed vertical displacement reaches compression, the out-of-plane deformation has been completely recovered, and the curvature profile becomes almost null (magenta triangles in Fig. 1b to e).

The reference model has been used in order to study the sensitivity of the out-of-plane response with respect to several parameters [12]: (i) Loading protocol: different values of maximum tensile positive displacement have been imposed, showing that the corresponding plastic deformation controls the maximum value of out-of-plane displacement attained upon reloading in compression. In fact, only when the reinforcement stiffness reduces considerably and the cracks are still open, large out-of-plane deformation can take place; (ii) Column thickness: several international codes allow building wall sections with a single layer of reinforcement and thickness as low as 80-100 mm [5]; the results of the numerical simulation have shown that, as expected, a thinner section is more susceptible to develop larger out-of-plane deformations.

3. Experimental results from the experimental tests of equivalent columns

Within a collaborative project involving the École Polytechnique Fédérale de Lausanne, the University of Valle, the EIA University and the University of Medellin, in Colombia, an experimental campaign on 12 equivalent RC thin columns (the specimens are named ‘TC’) with a single layer of vertical reinforcement is ongoing in the laboratory of the École Polytechnique Fédérale de Lausanne. The columns tested are representative of a full-scale boundary element of a thin wall. The experimental campaign is still in progress and only three columns have been tested so far [13]. These first three specimens (TC10, TC11 and TC12) were geometrically identical: the cross-section was 300 mm long and 100 mm thick (see Fig. 2a), and the reinforcement—placed in a single layer at an eccentricity of 8 mm with respect to the centerline of the section—consisted of three bars of diameter 16 mm (total longitudinal reinforcement ratio $\rho_c=2.01\%$). The horizontal reinforcement consisted of 16 bars of diameter 6 mm placed at a distance of 150 mm (reinforcement ratio $\rho_h=0.19\%$). The columns were 2.4 m high, while the foundation and the head were RC blocks designed as stiff rigid members. The concrete strengths were $f_c=33.6$ MPa and $f_c=32.9$ MPa for specimens TC10-11 and TC12 respectively, while the characteristics of the reinforcement were $f_y=515$ MPa and $f_u=620$ MPa, at yielding and rupture respectively.

The test was performed in deformation control. The vertical displacements imposed were evaluated averaging the measurements provided by four vertical LVDTs measuring the elongation along the four edges of the column. The three-dimensional displacement fields of the two shorter sides (North and South faces, see Fig. 2a) were recorded using an optical triangulation measurement system [14] through a grid of more than 180 infrared light emitting diodes (LEDs) glued to the surfaces. The LEDs were placed on the column—at a regular

distance of 40 mm in the horizontal direction and 100 mm in the vertical one, see Fig. 2b-c-d—on the top and on the foundation.

The loading protocol consisted of cyclic axial displacements. The peak displacements in the negative direction (compression) were always the same (-0.8 mm), corresponding to an average compressive strain of -0.033%. The peak displacements in the positive direction (tension) were increased every other cycle. The following positive peak displacements were applied: 1.5 mm → 3 mm → 6 mm → 9 mm → 12 mm → 15 mm → 18 mm for TC10-11, and 3 mm → 6 mm → 12 mm → 24 mm for TC12.

All the three specimens developed large out-of-plane deformations during loading, and the tests were stopped when out-of-plane failures were attained (see Fig. 2b-c-d), which means that the out-of-plane deformation was so large that concrete crushing in the plastic hinges took place and it was evident that the lateral displacement would not be recovered upon further increase of the compressive loads. All the specimens failed after having attained an average vertical tensile strain of 0.0075, corresponding to an applied vertical displacement of 18 mm (note that in TC12 the cycle at 18 mm was skipped, and the column failed after a vertical displacement of 21 mm). The last cycle in which the out-of-plane deformation was recovered corresponded to an average tensile strain of 0.005 for TC12 and 0.00625 for TC10-11. This suggests that the critical maximum tensile strain after which failure is attained lies between 0.00625 and 0.0075.

4. Comparison between experimental and numerical results of equivalent columns

The three specimens described in Section 3 were simulated using the numerical model described in Section 2, and the results were then compared with the experimental data.

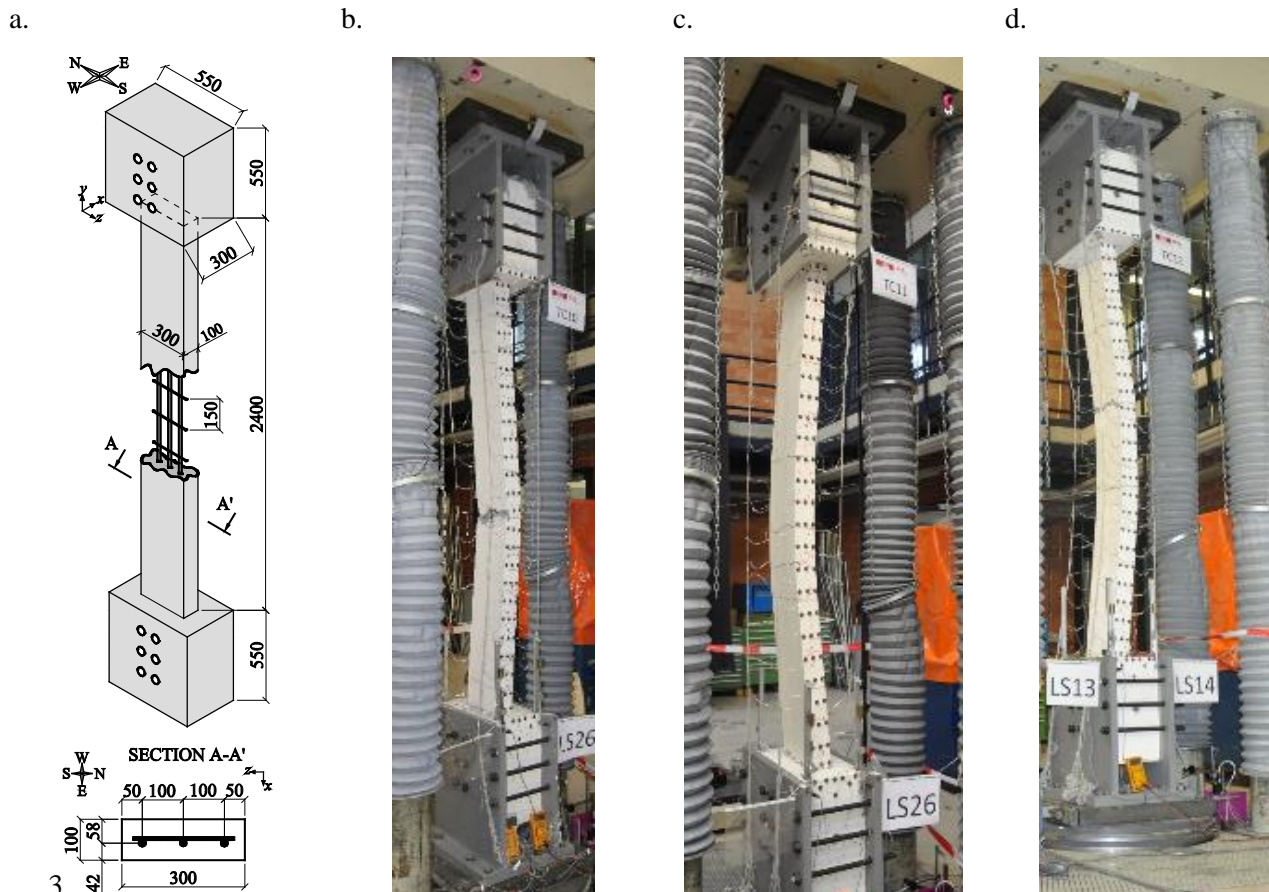


Fig. 2– a. Geometrical characteristics of columns TC10-11-12 (all dimensions in mm); View of the test setup and specimens after failure: b. TC10, c. TC11 d. TC12.

The columns were discretized using 26 elements along the height (the nodes were placed at the heights of the LEDs), the section was discretised into 16 concrete fibres, and each of the bars was discretised into four steel fibres. The concrete was modelled using an uniaxial Kent-Scott-Park law [15,16] with degrading linear unloading/reloading stiffness according to the work of Karsan-Jirsa [17] and zero tensile strength (concrete compressive strength $f'_c=33.3$ MPa, concrete compressive strain at maximum strength $\varepsilon_{c0}=0.002$), while the reinforcement was modelled considering an uniaxial Giuffrè-Menegotto-Pinto steel law [18,19] with isotropic strain hardening ($f'_y=515$ MPa, $E_s=205$ GPa and strain-hardening ratio $b=0.005$).

Since the specimens started to develop significant out-of-plane deformation after tensile displacements of 12 mm (equivalent to a tensile strain of 0.005), the reference model was initially subjected to this value of displacement, and then compressed up to a value of -0.8 mm. Only the cycles after which significant out-of-plane displacements were attained have been modelled.

Fig. 3a shows a comparison between the force-displacement curves obtained from the numerical simulation and from the experiments (only the first cycle at a tensile displacement of 12 mm is plotted, between a value of the vertical displacement equal to zero and the attainment of the compressive displacement targeted). A few differences between the curves can be pointed out. At the beginning of the curves (zero value of vertical displacement) the forces in the experiments are still negative (compression), and this behaviour can be related to the cyclic nature of the experiment. Just after having reached the maximum tensile displacement, in the experimental curves a small drop in the force can be observed: this is related to the fact that the test after each load stage was stopped for a certain period in order to take pictures and collect information on the crack development, and this break time caused a small reduction in the pressure of the pump of the testing machine and relaxation of the stresses in the rebars and concrete. Finally, the difference in the slope of the compressive branches can be related to the modelling of the concrete in the numerical simulation. In fact, since the concrete was assigned a zero tensile strength, until crack closure the only source of resistance comes from the steel rebars: this results in the underestimation of the compressive force until zero vertical displacement. Then at zero vertical displacement, in the model the cracks fully close along the column, causing a sudden increase in the compressive force. The equivalent increase in stiffness due to crack closure in the experimental curves is less evident since a more progressive phenomenon, affected by the roughness of the crack and small offsets along the crack, and an almost complete crack closure can be observed at around -300 kN.

Fig. 3d illustrates the out-of-plane displacement at the height where it was maximum (note that in the following we will refer to the out-of-plane displacement as the absolute value measured, not considering therefore if in the experiments the out-of-plane displacement occurred towards East or West) vs the average vertical strain imposed to the column. A first observation is that in the experiments the columns were slightly displacing out-of-plane also when they were subjected to a tensile displacement; then, upon reduction of the applied vertical displacement, the lateral deformations approached zero and just after attaining a compressive force the out-of-plane displacement started to increase again (the squares in Fig. 3a represent the beginning of the out-of-plane instability). It can also be noted that these deformations both in the experiments and in the numerical simulation started occurring almost at the same values of vertical displacement and compressive force.

The maximum out-of-plane displacement—represented by circles in Fig. 3a and Fig. 3d—is attained first in the model (black circle in Fig. 3a), while in the specimens tested it was reached for smaller values of vertical displacements and larger compressive forces. Moreover, the maximum value of out-of-plane displacement attained is larger in the numerical model (black circle in Fig. 3d), but still the lateral deformation is recovered, reproducing the experimental results. Concerning the height at which the maximum out-of-plane displacement was measured, Fig. 3g shows the out-of-plane profile along the height when the largest deformations throughout the cycle at 12 mm were attained. The maximum lateral displacement in the specimens occurred at very different heights (at 1100 mm above the foundation in TC10, 1400 mm in TC11, 2000 mm in TC12), while in the numerical model the maximum out-of-plane displacement is reached at midheight (1200 mm). However, the out-of-plane profile is captured acceptably well by the numerical model, in particular for the case of TC10 and TC11, whose deformed shape was more regular.

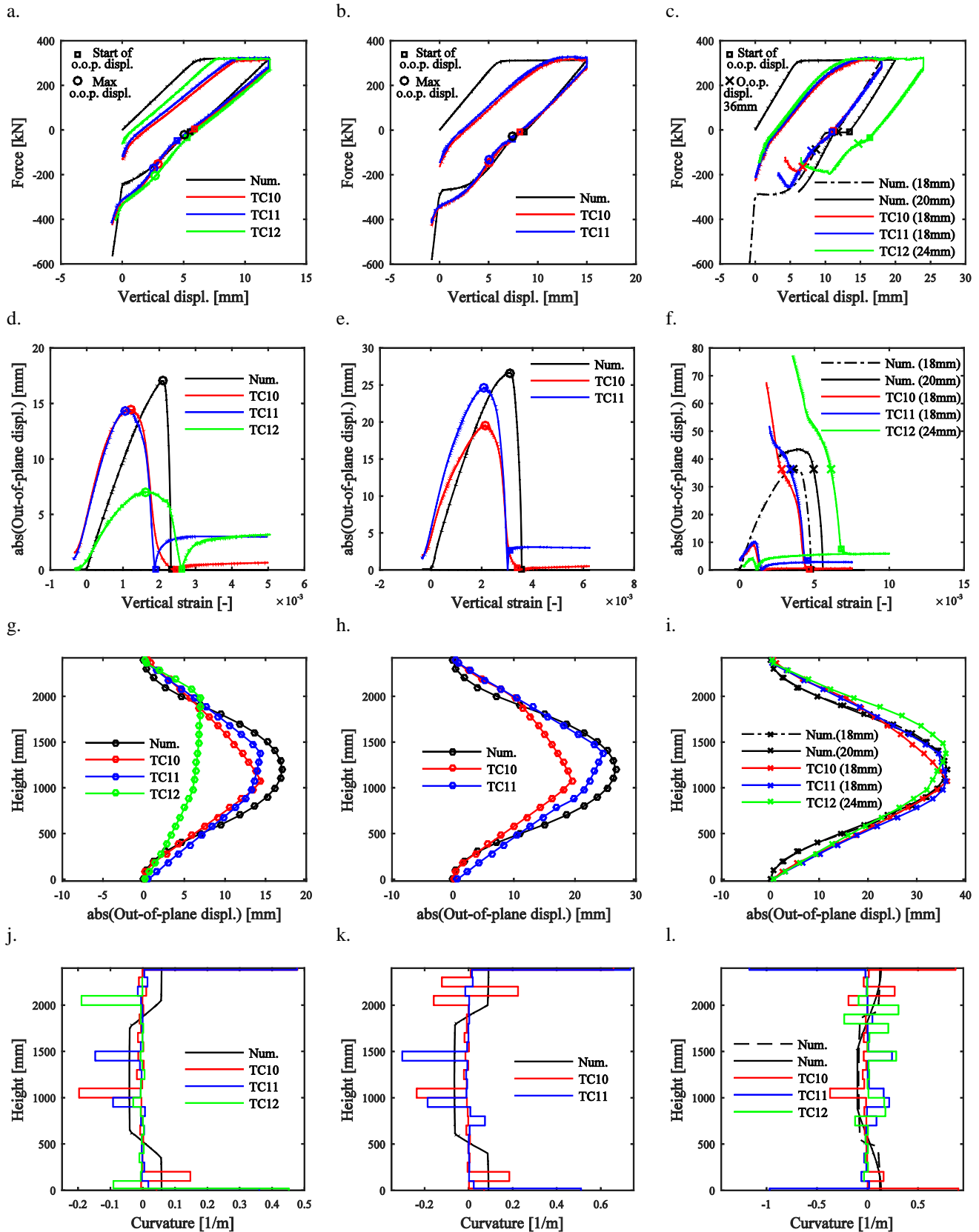


Fig. 3 – Force-displacement response (a-b-c), vertical strain vs out-of-plane at the height where it was maximum (d-e-f), out-of-plane profile along the height (g-h-i), and curvature profiles (j-k-l) in the cycles where 12 mm (a-d-g-j) or 15 mm (b-e-h-k) of vertical displacement were applied or in which failure was attained (c-f-i-l).

As a second analysis, the numerical reference model was subjected to a tensile displacement of 15 mm (tensile strain equal to 0.00625) and then compressed up to a value of -0.8 mm. Fig. 3b shows the force-displacement curves (only specimens TC10 and TC11 are presented, since for TC12 the cycle at 15 mm was skipped), and observations similar to the ones described above can be drawn. Fig. 3e shows that the numerical model again overestimates the maximum out-of-plane displacement. It can be noted that TC11 attained a larger lateral deformation than TC10, but the maximum occurred at very similar values in terms of force and vertical displacement (blue and red circles in Fig. 3b). Considering the out-of-plane profile (Fig. 3h), we can observe that at the base, specimen TC11 seems to have already formed a plastic hinge, while TC10 follows more the shape of the numerical model, while on top both specimens seem to have developed a hinge.

As a third analysis, the numerical reference model was subjected to a tensile displacement of 18 mm (tensile strain equal to 0.0075), which represents the value after which out-of-plane failure was attained in the experiments. In the numerical model this tensile displacement does not represent the critical one, since the out-of-plane deformation can still be recovered (see Fig. 3f). Therefore, the reference model was subjected to larger values of vertical displacement until out-of-plane failure of the column was obtained: this occurred when imposing a vertical displacement equal to 20 mm (corresponding to a tensile strain of 0.0083). Fig. 3f shows that in the numerical model after a tensile displacement of 20 mm, the out-of-plane deformation seems to recover but then failure is attained. Fig. 3i depicts the profiles of the lateral deformation along the height, at equivalent levels of maximum out-of-plane displacement (~36 mm, see Fig. 3f). The deformed shapes between the experiments and the simulations look very similar, but focussing on the extremities of the member it is clearly visible that the models still behave like a fix-fix column, while in the tests plastic hinges have formed.

Considering the rows of LEDs glued along the height of the column, strains along the thickness were computed in the experimental tests. Each one of the 25 row was formed by three LEDs—placed along the thickness at positions -40, 0 and 40 mm with respect to the centreline of the column—and the vertical distance between the rows was 100 mm. Subsequently, for each couple of rows, the three strain measures obtained along the thickness were interpolated linearly in order to obtain a continuous profile, and from these profiles the curvatures at the different heights were computed. In Fig. 3j-k and Fig. 3l the curvature profiles (at maximum out-of-plane deformation or at the same out-of-plane displacement before failure respectively) are compared with the results of the numerical simulations. In the experiments it is evident that the largest curvatures were concentrated at the heights where the plastic hinges formed, in particular at the extremities (the largest curvatures at the extremities can also be justified by the smaller gauge length, since the strains were computed using the rows of LEDs on the top and on the foundation and the first and last on the column). On the contrary, the numerical model uses distributed plasticity and more regular curvature profiles are obtained.

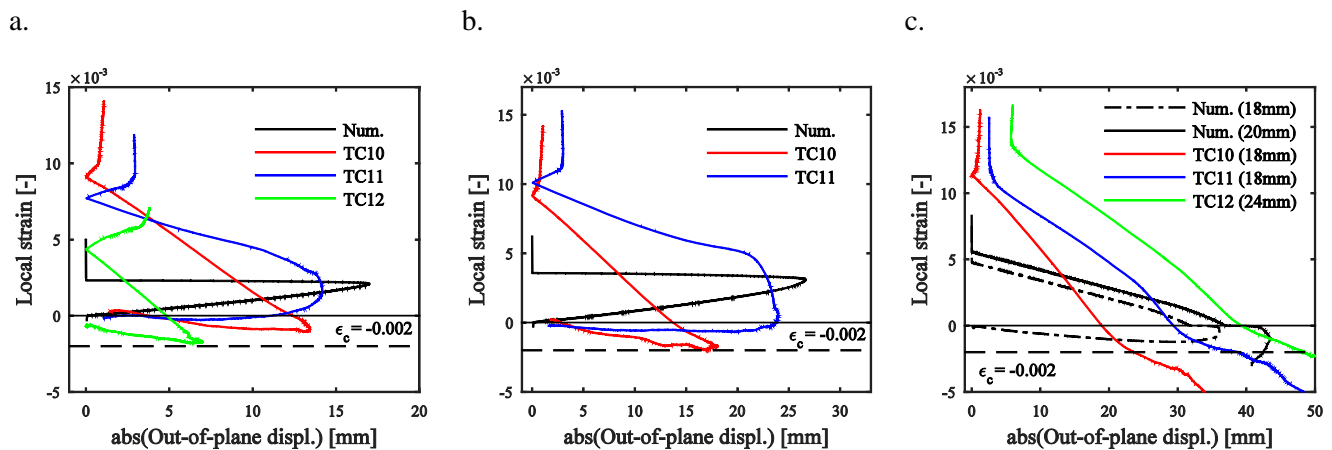


Fig. 4 – Out-of-plane displacement at the height where it was maximum vs local strain in the hinges, in the cycles at 12 mm (a) or 15 mm (b) of tensile displacement or in which failure was attained (c).

Finally, the experimental results and the numerical simulations are compared with regard to local strains in the region of the plastic hinges at midheight of the column. For the experiments the local vertical strains were computed from the two LEDs above and below the hinge, on the concave edge (intrados) of the out-of-plane deformed profile (i.e. on the edge along the thickness where the cracks first closed). For the numerical model, the strains were computed in the elements, which had the same length of the vertical spacing between the LEDs. Note that if in the experiments not one but two hinges formed at around midheight (TC11 and TC12), the strains were reported for that hinge that led to the larger strains.

The comparison of the local strains are plotted in Fig. 4. The three plots show the local strains vs the maximum out-of-plane displacement attained for the three analyses described above, in which the specimens and the numerical reference model were subjected to a tensile displacement of 12 mm (Fig. 4a), 15 mm (Fig. 4b), or in which failure was attained in the experiments (Fig. 4c). First of all, we can note that when we start unloading, at local level the vertical strains are much larger than the global tensile strain imposed to the specimens (i.e. 0.005 and 0.00625 in Fig. 4a and b respectively). This localized effect is not captured by the numerical model, in which the only source of resistance in tension is provided by the rebars, and therefore the local and the global vertical strains coincide. Secondly, a comparison of the three figures points out that a critical value of compressive strain equal to 0.002 is exceeded in the experiments only after having applied a tensile displacement of 18 mm (Fig. 4c). This value can be representative of the attainment of the peak resistance in the concrete and of the onset of crushing, therefore it seems that the onset of crushing prevents that the out-of-plane deformations are recovered [13]. A similar behaviour is observed for the numerical simulations: when a tensile displacement of 18 mm is applied, a compressive strain of 0.002 is not yet attained and the lateral deformation is recovered (black dash dot line in Fig. 4c); on the contrary, when 20 mm are imposed, the exceedance of this compressive strain leads to failure (black line in Fig. 4c). Hence, although further investigation is required, the attainment of local strains in compression larger than 0.002 appears to represent the critical condition defining the attainment of an out-of-plane failure also for the numerical model.

5. Comparison between experimental and numerical results of thin walls

The primary application of the beam-column model presented in this paper is to assess the vulnerability of walls to out-of-plane instability. In this context, the boundary element of a thin wall (TW1) tested at École Polytechnique Fédérale de Lausanne was simulated [20]. The specimen was a T-shaped wall, 2700 mm long and 2000 mm tall, tested with an equivalent shear span of 10 m. The cross-section of the boundary element was ~300 mm long and 80 mm thick, reinforced with three bars diameter of 16 mm, placed at an eccentricity of 4 mm with respect to the centerline of the section. The wall was subjected to quasi-static cyclic in-plane loading, and the out-of-plane deformations along the height were measured with an optical measurement system, using a grid of 255 LEDs glued on one of the long sides of the wall. The specimen failed due to an in-plane compressive failure which was triggered by damage induced by out-of-plane deformations.

In the numerical model, the boundary element was discretized along the height using an element every 100 mm, while the section was discretised into 16 concrete fibres and each of the bars into four steel fibres. The concrete and the reinforcement were modelled using the same laws described in Section 3 (the properties of the materials used were $f'_c=28.8$ MPa, $\epsilon_{c0}=0.002$, $f_y=565$ MPa, $E_s=205$ GPa and $b=0.005$ [20]). From the optical measurements the maximum value of tensile displacement experienced by the boundary element was derived, and the same value of tensile displacement was imposed to the numerical model (25.3 mm, see Fig. 5a). When applying this large strain of 0.01265 to the numerical model, an out-of-plane failure is attained (see Fig. 5b). The maximum tensile displacement impossible to the model in order to get a recovery of the lateral deformation is considerably lower, of 14.5 mm (equivalent to a tensile strain of 0.00725, see Fig. 5b). This difference is not surprising, since the approximation of the boundary element to an equivalent column does not take into account the restraints provided in reality by the rest of the wall. Fig. 5c compares the out-of-plane profile obtained experimentally with the ones obtained in the numerical simulations, at an equal value of 18.5 mm of maximum absolute out-of-plane displacement. The figure illustrates that in the experiment the maximum out-of-plane displacement was attained 755 mm above the foundation, and not at midheight as it obviously occurs in the numerical models. The reason of this asymmetry can be related to: (i) The presence of a moment gradient in the

wall: this forces the plastic deformations to take place at the base. A more representative equivalent beam-column model should hence apply a distributed axial force along the member height. (ii) The boundary conditions: in the experiment the out-of-plane displacements at the storey height were restrained only by four steel tubes, therefore these were not providing the same stiffness of the foundation at the base.

In order to try different simulation approaches, the boundary element was then modeled assuming an height of the column equal to the plastic hinge (PH) length of the wall. The latter, following the proposal by Paulay and Priestley [7], is equal to 980 mm. Fig. 5a-b show that this assumption leads to a maximum tensile strain that can be applied without attaining out-of-plane failure equal to 0.0154; this value is ~18% larger than the maximum tensile strain measured in the test. Fig. 5c illustrates the out-of-plane deformed shape, and it can be seen that the maximum lateral displacement (corresponding to 18.5 mm) is attained at midheight, i.e., at 500 mm, as expected.

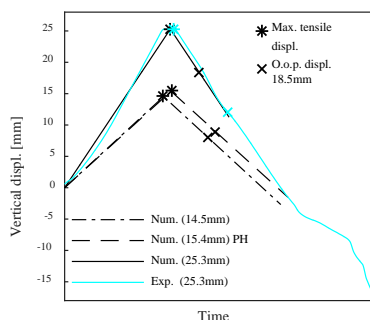
The results of this preliminary simulations show that modelling the boundary element of a real wall using the beam-column model leads, as anticipated, to an underestimation of the maximum tensile strain after which out-of-plane failure is attained, since the significant restraining effect that the rest of the wall exerts on the buckling region is neglected. Modeling the boundary element assuming a height equal to the plastic hinge length appears to provide more reasonable estimates of the critical tensile strain, although a final validation is not possible since the RC wall did not fail due to pure out-of-plane instability.

6. Conclusions and future work

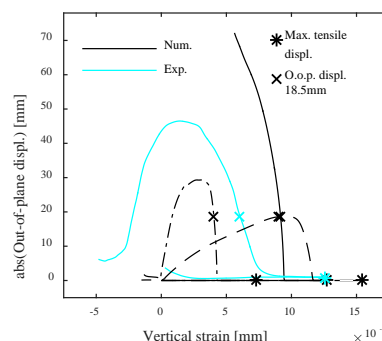
Many of the new residential buildings constructed in Latin America countries are built with very thin RC walls and a light amount of reinforcing steel, and these members can be vulnerable to out-of-plane instability. The existing models developed to describe the out-of-plane buckling of RC walls assimilate the boundary element—which represents the part of the wall mainly involved in the instability mechanism—to an equivalent column axially loaded in tension and compression. The parameter that governs the occurrence of out-of-plane deformations was identified as the magnitude of the maximum applied tensile strain prior to subsequent loading in compression. In order to investigate more in detail the out-of-plane instability mechanism, as well as to create design and assessment tools, the development of efficient modelling techniques is required.

This paper presents the application of a beam-column model—which uses a force-based element formulation with discretization of the sections in fibres—to simulate the out-of-plane behaviour of thin RC members. First, its response under tension-compression loading was described qualitatively in detail. Secondly, the preliminary results of an experimental campaign ongoing at École Polytechnique Fédérale de Lausanne were briefly presented; three thin RC columns with a single layer of vertical reinforcement were tested under cyclic tensile-compressive displacements. The simulation accuracy was assessed by comparison against the results obtained from this campaign. Finally, the beam-column model was used to simulate the behaviour of the boundary element of a thin wall tested in another experimental programme.

a.



b.



c.

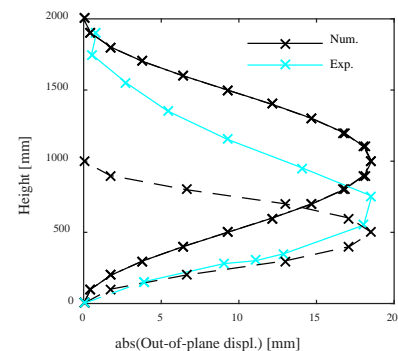


Fig. 5 – a. Vertical displacement measurement in the test and displacement histories imposed to the numerical models; b. vertical strain vs out-of-plane (o.o.p.) displacement at the height where it was maximum; c. out-of-plane deformed shapes for an absolute maximum out-of-plane of 18.5 mm.

A comparison between the numerical and the experimental results on thin RC columns showed that the use of the beam-column model can provide a slightly non-conservative estimate of the experimentally obtained maximum tensile strain causing an out-of-plane failure, together with a slightly overestimation of the maximum out-of-plane displacement attained. The overall qualitative and quantitative behaviour is well captured by the numerical model. Focussing then on the local strains, it was observed that a critical value of compressive strain equal to 0.002 was exceeded only just before attaining the out-of-plane failure, both in the experiments and in the numerical model. Further investigation is required, but the attainment of this value of local compressive strains seems to represent the critical condition defining the recoverability of out-of-plane instability.

Finally, the numerical model was used to simulate the boundary element of a thin wall tested in the past. The results showed that modeling the equivalent column leads to quite conservative estimates of the maximum tensile strain after which out-of-plane failure is expected, and hence the additional restraints imposed by the rest of the wall should be included in future models of equivalent columns. The numerical model will be further validated using future results of ongoing experimental campaigns [13], as well as of past tests on thin walls [5]. The development of mechanical models that capture the physics of the phenomena and can be straightforwardly used in the design or assessment of thin walls are also underway.

7. Acknowledgements

The testing of the specimens is financed through an EPFL Seed Money grant through the EPFL Cooperation & Development Center, which was awarded to the EESD Laboratory (PI), the University of Valle, the EIA University and the University of Medellin, in Colombia (Co-PIs). The first author is supported by the Swiss National Science Foundation. All contributions are gratefully acknowledged.

8. References

- [1] Wallace, J.W., Massone, L.M., Bonelli, P., Dragovich, J., Lagos, R., Lüders, C. et al. (2012) Damage and Implications for Seismic Design of RC Structural Wall Buildings. *Earthquake Spectra*, **28**, S281–99.
- [2] Kam, W.Y., Pampanin, S. and Elwood, K. (2011) Seismic performance of reinforced concrete buildings in the 22 February Christchurch (Lyttleton) earthquake. *Bulletin of the New Zealand National Society for Earthquake Engineering*, **44**, 239–78.
- [3] Sritharan, S., Beyer, K., Henry, R.S., Chai, Y.H., Kowalsky, H. and Bull, D. (2014) Understanding poor seismic performance of concrete walls and design implications. *Earthquake Spectra*, **30**, 307–34.
- [4] NIST. (2014) Recommendations for Seismic Design of Reinforced Concrete Wall Buildings Based on Studies of the 2010 Maule, Chile Earthquake. National Institute of Standards and Technology, U.S. Department of Commerce.
- [5] Rosso, A., Almeida, J.P. and Beyer, K. (2016) Stability of thin reinforced concrete walls under cyclic loads: state-of-the-art and new experimental findings. *Bulletin of Earthquake Engineering*, **14**, 455–84.
- [6] Goodsir, W.J. (1985) The design of coupled frame-wall structures for seismic actions. PhD Thesis. University of Canterbury, Christchurch, New Zealand.
- [7] Paulay, T. and Priestley, M.J.N. (1993) Stability of ductile structural walls. *ACI Structural Journal*, **90**, 385–92.
- [8] Chai, Y.H. and Elayer, D.T. (1999) Lateral stability of reinforced concrete columns under axial reversed cyclic tension and compression. *ACI Structural Journal*, **96**, 1–10.
- [9] Paulay, T. and Goodsir, W.J. (1985) The ductility of structural walls. *Bulletin of the New Zealand National Society for Earthquake Engineering*, **18**, 250–69.
- [10] McKenna, F., Fenves, G.L., Scott, M.H. and Jeremic, B. (2000) Open System for Earthquake Engineering Simulation (OpenSees). Pacific Earthquake Engineering Research Center, University of California, Berkeley, U.S.

- [11] Johnson, B. (2010) Anchorage detailing effects on lateral deformation components of RC shear walls. MSc Thesis. University of Minnesota, Minneapolis, U.S.
- [12] Rosso, A., Almeida, J.P. and Beyer, K. (2016) Out-of-plane behaviour of reinforced concrete members with single reinforcement layer subjected to cyclic axial loading: beam-column element simulation. *2016 NZSEE Conference*, Christchurch, New Zealand.
- [13] Rosso, A., Almeida, J.P., Jimenez, L., Guerrero, Z.P., Blandon, C., Bonett-Díaz, R. et al. (2016) Experimental tests on the out-of-plane response of RC columns subjected to cyclic tensile-compressive loading. *16th World Conference on Earthquake Engineering*, Santiago, Chile.
- [14] NDI. (2009) Optotrak Certus HD, Northern Digital Inc. [Internet]. <http://www.ndigital.com/industrial/certushd.php>, Waterloo, Ontario, Canada.
- [15] Kent, D.C. and Park, R. (1971) Flexural members with confined concrete. *Journal of the Structural Division, ASCE*, **97**, 1969–90.
- [16] Scott, B.D., Park, R. and Priestley, M.J.N. (1982) Stress-Strain Behavior of Concrete Confined by Overlapping Hoops at Low and High Strain Rates. *ACI Journal*, **79**, 13–27.
- [17] Karsan, I.D. and Jirsa, J.O. (1969) Behavior of Concrete Columns with Double-Head Studs Under Earthquake Loading: Parametric Study. *ASCE Journal of Structural Division*, **95**, 2543–63.
- [18] Giuffrè, A. and Pinto, P.E. (1970) Il comportamento del cemento armato per sollecitazioni cicliche di forte intensità. *Giornale Del Genio Civile*, **5**.
- [19] Menegotto, M. and Pinto, P.E. (1973) Method of analysis for cyclically loaded reinforced concrete plane frames including changes in geometry and nonelastic behaviour of elements under combined normal force and bending. *IABSE Symposium on Resistance and Ultimate Deformability of Structures Acted on by Well Defined Repeated Loads*, Lisbon.
- [20] Almeida, J.P., Prodan, O., Rosso, A. and Beyer, K. (2016) Tests on thin reinforced concrete walls subjected to in-plane and out-of-plane cyclic loading. *Earthquake Spectra*, manuscript submitted.